DOI: 10.1002/ejic.200600553

A Facile Hydrothermal Route to Flower-Like Cobalt Hydroxide and Oxide

Li-Xia Yang,[a,b] Ying-Jie Zhu,*[a] Liang Li,[a,b] Ling Zhang,[a,b] Hua Tong,[a,b] Wei-Wei Wang,[a,b] Guo-Feng Cheng,[a] and Jie-Fang Zhu[a]

Keywords: Cobalt hydroxide / Cobalt oxide / Materials science / Nanostructures / Solvothermal synthesis

Flower-like cobalt hydroxide [β-$Co(OH)_2$] consisting of nanosheet networks has been synthesized by a hydrothermal method from $Co(CH_3COO)_2{\cdot}4H_2O$ in mixtures of water and glycerol/ethylene glycol at 200 °C. The morphology and phase of the cobalt hydroxide can be controlled by adjusting the experimental parameters that include cobalt acetate concentration and the volume ratio of water to glycerol/ethylene glycol. The possible formation mechanism of flower-like cobalt hydroxide is discussed on the basis of experimental results. Cobalt oxide (Co_3O_4) flowers have also been obtained by thermal decomposition of cobalt hydroxide flowers in air at 400 °C. The products were characterized by powder XRD, TEM, selected-area electron diffraction (SAED), high resolution TEM (HRTEM), and field-emission SEM (FESEM).

Introduction

Research into nanomaterials has increased recently due to their unique electrical, optical, magnetic, and catalytic characteristics in comparison with the bulk materials. Currently, inorganic architectures with a hierarchical structure based on nano units and their specific properties for applications are attracting much interest in materials chemistry.[1–5] For example, the mediator-template assembly of gold nanoparticles into size-controllable nanostructures has been reported.[1] The interesting morphological and optical properties of these nanoparticle assemblies could potentially be exploited for optical sensing applications.[1] CoPt nanopolypods derived from the assembly of nanorods have been synthesized by a simple and large-scale-applicable thermolytic reaction,[2] and high-order superstructures of zeolite doughnuts with nanoscale building blocks (sheet-like discs) have been synthesized by a synergic dual-template method in a one-pot reaction.[3] The controlled construction of primary building blocks into curved structures provides another challenge for materials synthesis because of their potential use in new technological applications.

Cobalt hydroxide [$Co(OH)_2$] has recently received increasing attention due to its important technological applications. For example, cobalt hydroxide is usually added to nickel hydroxide electrodes to enhance the electrode conductivity and chargeability,[6,7] and composite materials of cobalt hydroxide and ultra-stable Y zeolite molecular sieves have shown potential applications in electrochemical capacitors.[8] Cobalt hydroxide films show catalytic and reversible electrochromic properties.[9,10] In particular, Kurmoo has reported the incorporation of different anions into the interlayers of cobalt hydroxide to form organic magnetic materials.[11] The preparation of single-crystalline β-$Co(OH)_2$ nanosheets is easily achieved because of their intrinsic lamellar structures.[12–14] However, there are few reports on the formation of 3D β-$Co(OH)_2$ architectures assembled from nanostructures, except the butterfly-like nanocrystals of β-$Co(OH)_2$ prepared by an ethylenediamine-mediated route.[15] At present, the synthesis of β-$Co(OH)_2$ hierarchical nanostructures is still a big challenge for researchers.

Spinel cobalt oxide (Co_3O_4), which is an important p-type semiconductor, has potential applications in sensors, lithium-ion batteries, and catalysis.[16–19] Furthermore, Co_3O_4 nanoparticles show interesting magnetic and field-emission properties.[20,21] There have been some reports on the synthesis of cobalt oxide nanocubes, nanorods, nanotubes, hollow spheres, and nanoboxes.[22–27] However, to the best of our knowledge, there has been no report on the synthesis of Co_3O_4 flowers consisting of nanosheet building blocks.

Here we report a simple hydrothermal approach to the synthesis of two kinds of β-$Co(OH)_2$ flowers consisting of nanosheet building blocks by the hydrolysis of cobalt acetate in solvent mixtures containing a polyalcohol and deionized water. Co_3O_4 flowers are readily obtained by thermal decomposition of $Co(OH)_2$ flowers in air. These β-$Co(OH)_2$ and Co_3O_4 flowers are expected to have potential applications in sensors, batteries, and catalysis.

[a] State Key Laboratory of High Performance Ceramics and Superfine Microstructure, Shanghai Institute of Ceramics, Chinese Academy of Sciences,
Shanghai 200050, P. R. China
Fax: +86-21-5241-3122
E-mail: y.j.zhu@mail.sic.ac.cn
[b] Graduate School of Chinese Academy of Sciences, P. R. China

Results and Discussion

The phase of the as-prepared sample was examined by XRD. Figure 1(a) shows the XRD pattern of sample 1 prepared in a mixture of water and glycerol. All diffraction peaks in this pattern can be indexed as a single phase of the hexagonal brucite-like β-$Co(OH)_2$, which is consistent with the values in the literature (JCPDS no. 74-1057). The typical FESEM micrographs shown in Figure 1b–d reveal that sample 1 consists of relatively uniform flower-like structures. Each flower-like structure is composed of a network of nanosheet building blocks. The sizes of these flowers are in the range 6–9 μm, and the thickness of the nanosheets is less than 100 nm. The above results demonstrate that β-$Co(OH)_2$ with a flower-like morphology can be produced using the present synthetic scheme.

It is believed that the physical and chemical properties of the solvent can influence the solubility, reactivity, and diffusion behavior of the reagents and the intermediate.[28] In our reaction system, the properties of the mixed solvents can be easily adjusted by varying the volume ratio of glycerol to water. The volume ratio of glycerol to water (V_g/V_w) has a great influence on the formation of the product. As discussed above, a single phase of hexagonal β-$Co(OH)_2$ was obtained when V_g/V_w was 1:3 (sample 1). When V_g/V_w was adjusted to 1:6.5, however, a mixture of Co_3O_4 and β-$Co(OH)_2$ was obtained at 200 °C after 10.5 h [sample 2, Figure 2(a)]. When the reaction time was prolonged to 24.5 h (sample 3), a single phase of β-$Co(OH)_2$ was obtained (Figure 2b), thus indicating that glycerol can act as a reducing agent to reduce Co^{3+} to Co^{2+}, which results in the transformation of Co_3O_4 to $Co(OH)_2$. Compared with the reaction with V_g/V_w = 1:3, it takes a relatively longer time to form a single phase of β-$Co(OH)_2$ when using less glycerol. We also studied the effect of cobalt acetate concentration on the product, with a constant V_g/V_w ratio of 1:3. When the amount of cobalt acetate was decreased to 0.100 g, a single phase of β-$Co(OH)_2$ with a pink color was still obtained (sample 4). However, if more cobalt acetate was used (1.000 g, sample 5), the product was blue, similar to that of α-$Co(OH)_2$, although the XRD pattern (Figure 2c) cannot be indexed to that of α-$Co(OH)_2$.

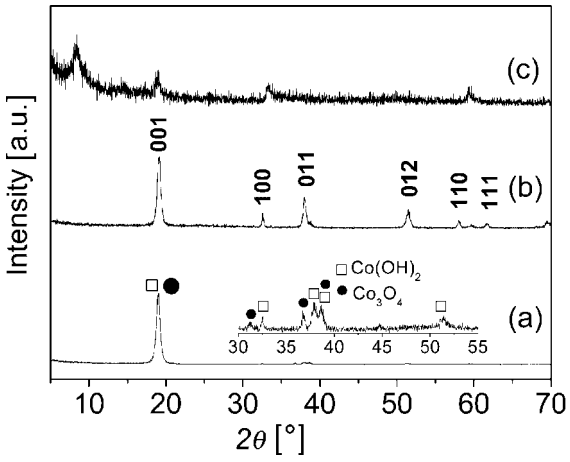

Figure 2. XRD patterns of different samples prepared by hydrothermal treatment at 200 °C: (a) sample 2; (b) sample 3; (c) sample 5.

In order to understand the formation process of β-$Co(OH)_2$ flowers, the morphologies of samples 3 and 4 were also examined by FESEM. When using less cobalt acetate (sample 4, Figure 3a), imperfect flowers assembled from

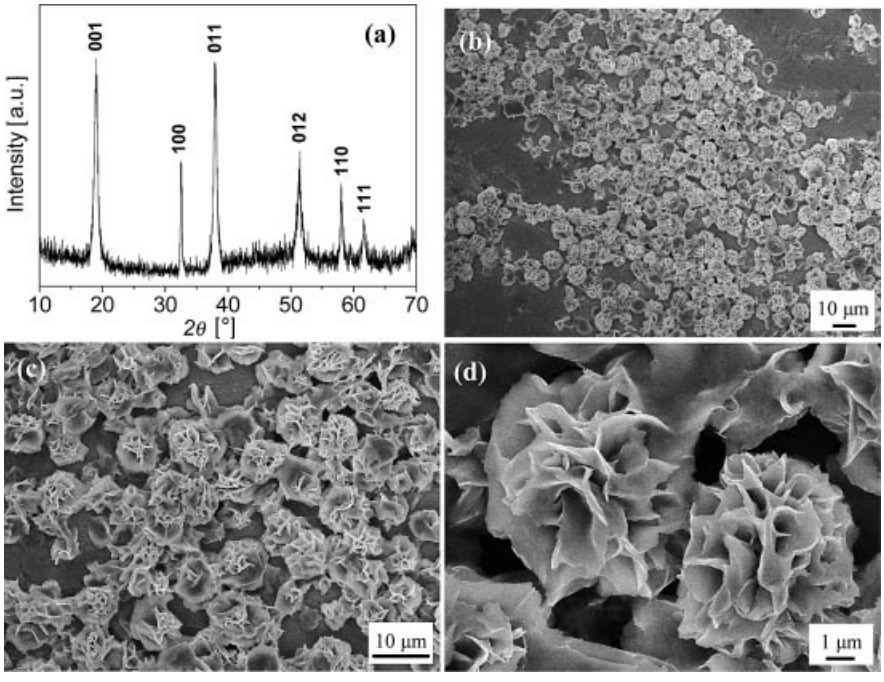

Figure 1. (a) XRD pattern of the obtained β-$Co(OH)_2$ (sample 1); (b–d) FESEM micrographs of β-$Co(OH)_2$ flowers (sample 1) at different magnifications.

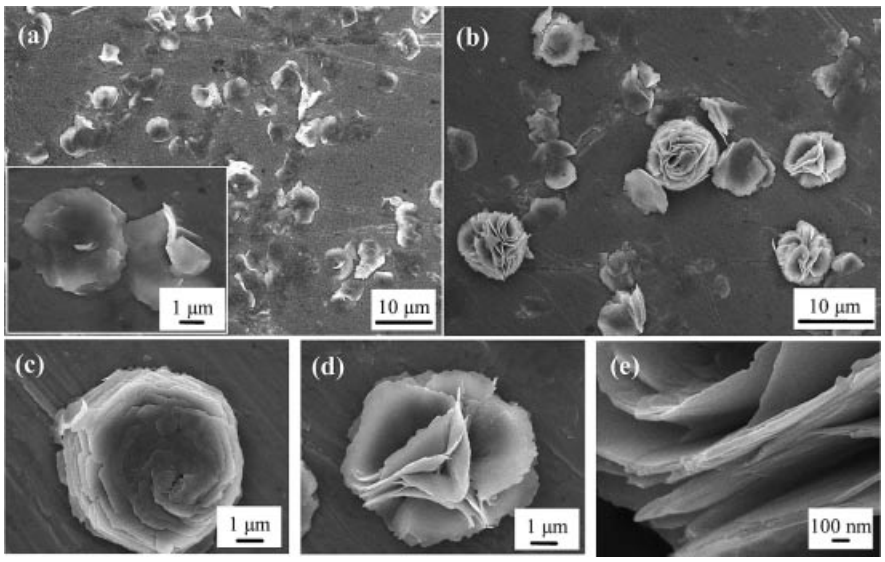

Figure 3. (a) FESEM micrograph of sample 4; (b) FESEM micrograph of sample 3; (c) and (d) FESEM micrographs of single flowers in sample 3; (e) a magnified FESEM micrograph of a flower in sample 3.

nanosheets were observed with dimensions below 7.5 μm, along with a few single nanosheets. The number of petals in these flowers is less than those in sample 1, as shown in Figure 3a. Upon decreasing the volume of glycerol, sample 3 shows a mixed morphology of nanosheets and flowers. Two kinds of flowers are observed, as shown in Figures 3c and 3d, which show that one kind of flower consists of flat nanosheets and the other of curved nanosheets. The morphology in Figure 3c was not observed in sample 1, so we suggest that it is due to the lower volume of glycerol used. The thickness of the nanosheets in the flowers was estimated to be below 50 nm (Figure 3e).

Ethylene glycol (EG) was also used as a co-solvent to substitute glycerol in order to understand the formation mechanism of the β-$Co(OH)_2$ flowers. The same experimental conditions as for the formation of sample 1 were adopted except for the use of EG instead of glycerol, and a mixture of β-$Co(OH)_2$ and Co_3O_4 was obtained, thereby illustrating that EG cannot completely reduce Co^{3+} to Co^{2+} at 200 °C after 10.5 h. A single phase of β-$Co(OH)_2$ was obtained upon increasing the volume ratio of EG to water and prolonging the reaction time to 20.5 h (sample 6, Figure 4a). Surprisingly, a different kind of flower was observed, as shown in the FESEM micrographs of sample 6 (Figure 4). The β-$Co(OH)_2$ flowers look like carnations consisting of curved nanosheet building blocks. These carnations have sizes in the range 5–15 μm.

On the basis of the above results, we can propose a formation mechanism for the β-$Co(OH)_2$ flowers. First, the hydrolysis of cobalt acetate results in the formation of OH^- ions ($CH_3COO^- + H_2O \rightarrow CH_3COOH + OH^-$), which provide a basic environment for the formation of cobalt hydroxide. Sheet-like $Co(OH)_2$ forms as a general morphology due to its layered structure. In addition, glycerol/EG can act as a reducing agent. In the absence of glycerol or EG, only Co_3O_4 nanocubes are obtained. Co_3O_4 is formed by the oxidation of β-$Co(OH)_2$ by oxygen in the autoclave and is then reduced by glycerol/EG to form a single phase of β-$Co(OH)_2$. Besides acting as a reducing agent, glycerol/EG could coordinate to the cobalt ions to form complexes in solution,[29,30] which decreases the free Co^{2+} concentration in solution and results in the slow generation of β-$Co(OH)_2$. This coordination between cobalt ions and glycerol/EG may be favorable for the formation of the flower nuclei,

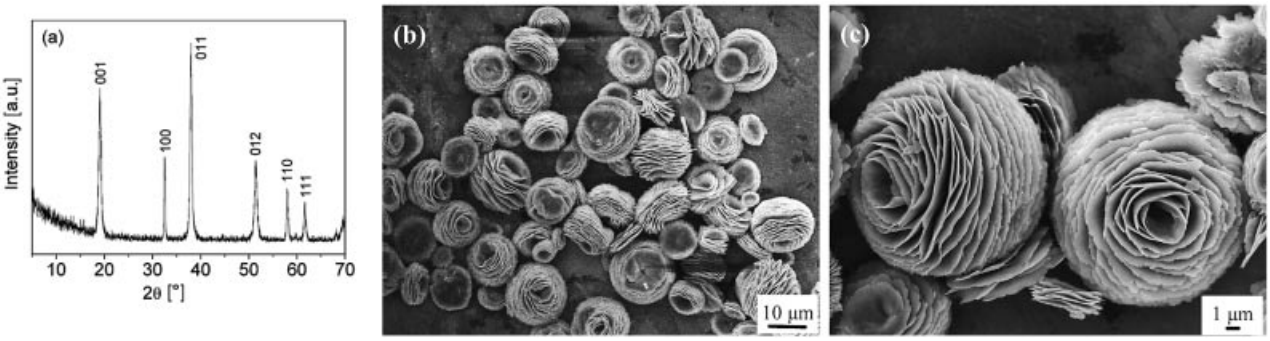

Figure 4. (a) XRD pattern of sample 6; (b) and (c) FESEM micrographs of sample 6 at different magnifications.

resulting in the formation of flower-like β-$Co(OH)_2$. Furthermore, glycerol helps to generate a highly viscous and stable mixture solution, which favors the stable growth of nanosheets and the formation of β-$Co(OH)_2$ flowers with nanosheets as building blocks. As discussed above, a higher V_g/V_w ratio favors the formation of flowers consisting of curved nanosheets instead of those with flat nanosheets (samples 1 and 3), thus indicating that the higher viscosity caused by glycerol can prohibit the aggregation of nanosheets and promotes the formation of flowers with curved nanosheets. Qian et al.[31] have reported the synthesis of copper nanowires by a complex-surfactant-assisted hydrothermal reduction process in a mixture of water and glycerol. The high viscosity shows a good effect on prohibiting the aggregation of copper particles and results in a relatively stable suspension. One of the keys to the formation of these flower structures is the use of cobalt acetate as the cobalt source without the addition of any base. The slower hydrolysis of acetate and the complexation of cobalt ions with glycerol/EG are favorable for the formation of these superstructures. In the presence of glycerol, when NaOH is added to the solution (sample 7), only irregular nanosheets are formed (Figure 5). Although glycerol provides a viscous environment, the introduction of a strong base (NaOH) could accelerate the reaction and prevent the formation of flowers. However, in the presence of EG, the viscosity is not as high as with glycerol, therefore the nanosheets tend to self-assemble to reduce the surface energy in the mixture of EG and water, and follows a layer-by-layer growth style so that hierarchical carnation structures are formed.

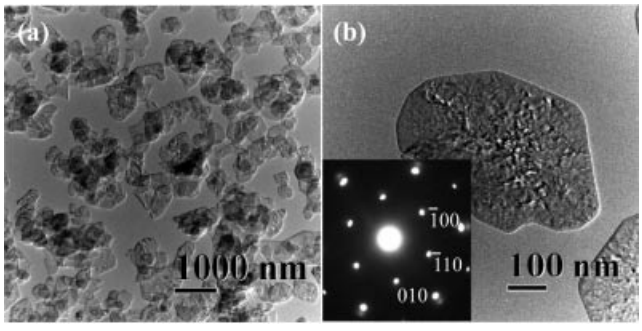

Figure 5. (a, b) TEM micrographs of the obtained β-$Co(OH)_2$ nanosheets of sample 7; the inset of (b) is the corresponding SAED pattern.

TEM was used to study the crystal structure of β-$Co(OH)_2$. Figure 6a shows a single nanosheet of sample 4. The SAED pattern (Figure 6b) of this nanosheet exhibits a hexagonal symmetry, thus indicating that the surface of the nanosheet is the $(00\bar{1})$ plane of β-$Co(OH)_2$, and the direction along the thickness of the obtained β-$Co(OH)_2$ is $[00\bar{1}$; the *c* axis of hexagonal β-$Co(OH)_2$]. The SAED pattern changes rapidly under electron irradiation to give another set of diffraction patterns that are close to the original one that show elongated diffraction spots rather than bright dots, thereby indicating the coexistence of two different species (Figure 6c). The inner set of hexagonal diffraction spots is still due to β-$Co(OH)_2$, and the outer set of diffraction spots corresponds to CoOOH. The electron beam is also along the $[00\bar{1}]$ direction of hexagonal CoOOH (JCPDS no. 26-1107). A similar SAED pattern has been reported for a mixture of β-$Co(OH)_2$ and CoOOH.[32] The diffraction pattern of β-$Co(OH)_2$ vanishes after prolonged irradiation by the electron beam and another set of SAED patterns (Figure 6d) is obtained, which shows the coexistence of CoOOH and Co_3O_4. The diffraction dots indicated by the white arrows show a hexagonal symmetry and can be indexed to the SAED pattern of a cubic Co_3O_4 phase (JCPDS no. 80-1541) with the incident electron beam along the [111] direction. This phenomenon implies that the thin β-$Co(OH)_2$ nanosheets synthesized using the current method are not stable under electron beam irradiation and that prolonged exposure of the sample to the electron beam during the TEM observation will destroy the structure of β-$Co(OH)_2$, resulting in the formation of Co_3O_4 nanoparticles with sizes of 1–4 nm, as shown in the high-resolution TEM (HRTEM) image of Figure 6e. The interplanar dis-

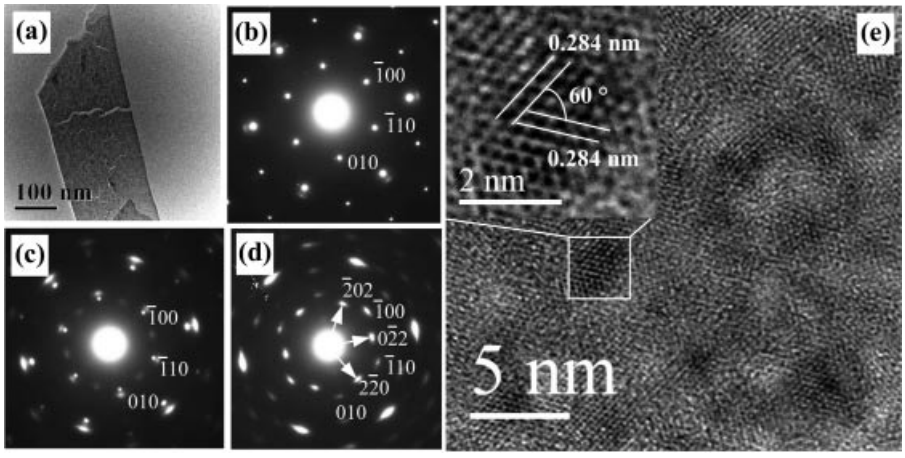

Figure 6. (a) TEM micrograph of an individual β-$Co(OH)_2$ nanosheet of sample 4; (b–d) the corresponding SAED patterns taken at different irradiation times; (e) HRTEM image taken of the individual nanosheet corresponding to the SAED pattern of (d).

tance of the crystal fringes with an angle of 60° is 2.84 nm, which is consistent with the $(\bar{2}02)$ and $(0\bar{2}2)$ planes of a cubic Co_3O_4 phase.

Co_3O_4 is obtained by thermal conversion of the β-$Co(OH)_2$ flower precursor at 400 °C after 3 h. Figure 7 shows the XRD pattern of the product. All the diffraction peaks can be indexed to a single phase of a cubic Co_3O_4, which matches well with the reported data (JCPDS no. 80-1541). No peaks from the β-$Co(OH)_2$ precursor are observed in the XRD pattern, thus indicating the complete transformation of β-$Co(OH)_2$ to Co_3O_4.

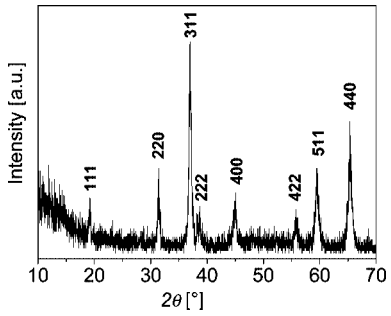

Figure 7. XRD pattern of Co_3O_4 (sample C1).

After the thermal conversion from β-$Co(OH)_2$ to Co_3O_4, the two kinds of flower-like morphology of β-$Co(OH)_2$ were almost sustained and Co_3O_4 flowers were obtained. In addition, a few single nanosheets were also observed, as shown in Figure 8a,b. A single nanosheet is shown in Figure 8c, from which one can see that the surface of this nanosheet is not smooth. The SAED pattern of this nanosheet, which was taken by focusing the incident electron beam along the [111] zone axis, reveals a single crystal structure that can be indexed to cubic Co_3O_4, consistent with the XRD results. The HRTEM image of the nanosheet shows that the spacing between clear lattice fringes with an angle of 60° is 0.284 nm, which is consistent with the $(\bar{2}02)$ and $(0\bar{2}2)$ planes of a cubic Co_3O_4.

Conclusions

We have demonstrated a facile strategy to synthesize two kinds of β-$Co(OH)_2$ flowers consisting of nanosheets as the building unit. Glycerol or ethylene glycol serves as a co-solvent and also a reducing agent in this reaction system. Both the volume ratio of glycerol/EG to water and the concentration of cobalt acetate affect the phase and morphology of the product. Co_3O_4 flowers can be obtained by a simple thermal conversion of the β-$Co(OH)_2$ flower precursor in air; the flower-like morphology can be preserved during the thermal conversion process. β-$Co(OH)_2$ nanosheets are not stable under electron beam irradiation and are transformed into CoOOH and Co_3O_4. This simple synthetic method, which does not use any surfactant or template, may be extended to the synthesis of other materials with novel morphologies.

Experimental Section

All reagents were of analytical grade and were purchased and used as received without further purification. In a typical procedure, cobalt acetate [$Co(CH_3COO)_2{\cdot}4H_2O$] (0.25 g) was dissolved in a mixture of deionized water and glycerol (30 mL) with a volume ratio

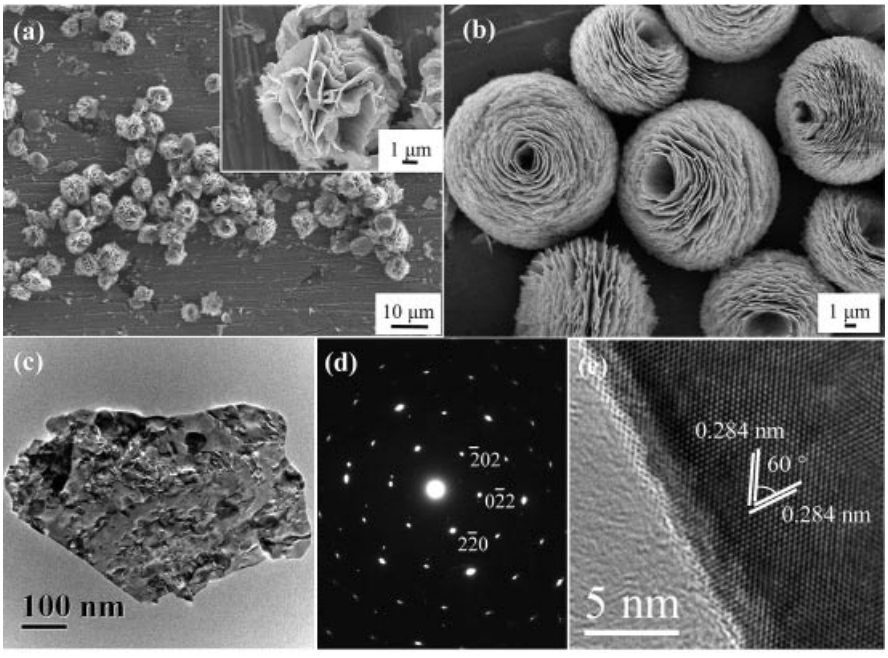

Figure 8. (a) FESEM micrograph of Co_3O_4 (sample C1); (b) FESEM micrograph of Co_3O_4 (sample C6); (c) TEM micrograph of an individual nanosheet (sample C1) and (d) the corresponding SAED pattern; (e) HRTEM image of this individual Co_3O_4 nanosheet.

Table 1. Detailed experimental parameters for the synthesis of some typical samples (at 200 °C for all samples).

Sample	Reaction system	Time [h]	Phase	Morphology
1	0.25 g $Co(CH_3COO)_2{\cdot}4H_2O$ + 7.5 mL glycerol + 22.5 mL H_2O	10.5	β-$Co(OH)_2$	flowers
2	0.25 g $Co(CH_3COO)_2{\cdot}4H_2O$ + 4 mL glycerol + 26 mL H_2O	10.5	β-$Co(OH)_2$ + Co_3O_4	–
3	0.25 g $Co(CH_3COO)_2{\cdot}4H_2O$ + 4 mL glycerol + 26 mL H_2O	24.5	β-$Co(OH)_2$	flowers and nanosheets
4	0.10 g $Co(CH_3COO)_2{\cdot}4H_2O$ + 7.5 mL glycerol + 22.5 mL H_2O	10.5	β-$Co(OH)_2$	imperfect flowers
5	1.00 g $Co(CH_3COO)_2{\cdot}4H_2O$ + 7.5 mL glycerol + 22.5 mL H_2O	10.5	unknown	–
6	0.25 g $Co(CH_3COO)_2{\cdot}4H_2O$ + 20 mL ethylene glycol + 10 mL H_2O	20.5	β-$Co(OH)_2$	carnations
7	0.25 g $Co(CH_3COO)_2{\cdot}4H_2O$ + 7.5 mL glycerol + 17.5 mL H_2O + 5 mL NaOH (1 M)	10.5	β-$Co(OH)_2$	nanosheets

of 3:1 at room temperature, and the solution was then transferred into a Teflon-lined, 40-mL autoclave and maintained at 200 °C for 10.5 h. It was then cooled to room temperature. This sample was denoted as sample 1. The product was then collected by centrifugation and washed with deionized water and absolute ethanol repeatedly, then dried in air at 60 °C. The detailed experimental parameters for the synthesis of some typical samples are listed in Table 1. Co_3O_4 samples were obtained by thermal decomposition of β-$Co(OH)_2$ flowers (samples 1 and 6) in a tubular oven at 400 °C after 3 h in air. The obtained Co_3O_4 samples are denoted as samples C1 and C6, respectively.

Powder XRD data were collected on a Rigaku D/max 2550 V X-ray diffractometer with high-intensity Cu-K_α radiation (λ = 1.54178 Å) and a graphite monochromator. The morphology was studied with a JEOL JSM-6700F field emission scanning electron microscope (FESEM). TEM, SAED, and HRTEM images were obtained using a JEOL JEM-2100F field emission transmission electron microscope.

Acknowledgments

Financial support from the National Natural Science Foundation of China (50472014), the Chinese Academy of Sciences under the Program for Recruiting Outstanding Overseas Chinese (Hundred Talents Program), and the Fund for Innovation Research from the Shanghai Institute of Ceramics is gratefully acknowledged. This work was also supported by the Program of the Shanghai Postdoctoral Scientific Research Foundation (05R214148), the Opening Project of the State Key Laboratory of High Performance Ceramics and Superfine Microstructure (SKL200506SIC), Shanghai Institute of Ceramics, Chinese Academy of Sciences.

[1] M. M. Maye, I. I. S. Lim, J. Luo, Z. Rab, D. Rabinovich, T. B. Liu, C. J. Zhong, *J. Am. Chem. Soc.* **2005**, *127*, 1519–1529.
[2] V. Tzitzios, D. Niarchos, M. Gjoka, N. Boukos, D. Petridis, *J. Am. Chem. Soc.* **2005**, *127*, 13756–13757.
[3] G. Hu, D. Ma, L. Liu, M. Cheng, X. H. Bao, *Angew. Chem. Int. Ed.* **2004**, *43*, 3452–3456.
[4] M. Mo, J. C. Yu, L. Z. Zhang, S. K. A. Li, *Adv. Mater.* **2005**, *17*, 756–760.
[5] B. Liu, S. H. Yu, L. Li, Q. Zhang, F. Zhang, K. Jiang, *Angew. Chem. Int. Ed.* **2004**, *43*, 4745–4750.
[6] W. Y. Li, S. Y. Zhang, J. Chen, *J. Phys. Chem. B* **2005**, *109*, 14025–14032.
[7] J. Ismail, M. F. Ahmed, P. V. Kamath, *J. Power Sources* **1993**, *41*, 223–230.
[8] L. Cao, F. Xu, Y. Y. Liang, H. L. Li, *Adv. Mater.* **2004**, *16*, 1853–1857.
[9] M. Dinamani, P. V. Kamath, *J. Appl. Electrochem.* **2000**, *30*, 1157–1161.
[10] N. Ozer, D. G. Chen, T. Buyuklimanli, *Sol. Energy Mater. Sol. Cells* **1998**, *52*, 223–230.
[11] M. Kurmoo, *Chem. Mater.* **1999**, *11*, 3370–3378.
[12] Y. L. Hou, H. Kondoh, M. Shimojo, T. Kogure, T. Ohta, *J. Phys. Chem. B* **2005**, *109*, 19094–19098.
[13] Z. P. Liu, R. Z. Ma, M. Osada, K. Takada, T. Sasaki, *J. Am. Chem. Soc.* **2005**, *127*, 13869–13874.
[14] Y. C. Zhu, H. L. Li, Y. Koltypin, A. Gedanken, *J. Mater. Chem.* **2002**, *12*, 729–733.
[15] J. T. Sampanthar, H. C. Zeng, *J. Am. Chem. Soc.* **2002**, *124*, 6668–6675.
[16] W. Y. Li, L. N. Xu, J. Chen, *Adv. Funct. Mater.* **2005**, *15*, 851–857.
[17] Y. M. Kang, M. S. Song, J. H. Kim, H. S. Kim, M. S. Park, J. Y. Lee, H. K. Liu, S. X. Dou, *Electrochim. Acta* **2005**, *50*, 3667–3673.
[18] J. Jansson, A. E. C. Palmqvist, E. Fridell, M. Skoglundh, L. Österlund, P. Thormählen, V. Langer, *J. Catal.* **2002**, *211*, 387–397.
[19] S. Fujita, K. Suzuki, T. Mori, *Catal. Lett.* **2003**, *86*, 139–144.
[20] C. Nethravathi, S. Sen, N. Ravishankar, M. Rajamathi, C. Pietzonka, B. Harbrecht, *J. Phys. Chem. B* **2005**, *109*, 11468–11472.
[21] T. Yu, Y. W. Zhu, X. J. Xu, Z. X. Shen, P. Chen, C. T. Lim, J. T. L. Thong, C. H. Sow, *Adv. Mater.* **2005**, *17*, 1595–1599.
[22] T. He, D. R. Chen, X. L. Jiao, Y. L. Wang, Y. Z. Duan, *Chem. Mater.* **2005**, *17*, 4023–4030.
[23] R. Xu, H. C. Zeng, *J. Phys. Chem. B* **2003**, *107*, 926–930.
[24] Y. K. Liu, G. H. Wang, C. K. Xu, W. Z. Wang, *Chem. Commun.* **2002**, 1486–1487.
[25] X. Y. Shi, S. B. Han, R. J. Sanedrin, F. Zhou, M. Selke, *Chem. Mater.* **2002**, *14*, 1897–1902.
[26] T. He, D. R. Chen, X. L. Jiao, Y. Y. Xu, Y. X. Gu, *Langmuir* **2004**, *20*, 8404–8408.
[27] T. He, D. R. Chen, X. L. Jiao, Y. L. Wang, *Adv. Mater.* **2006**, *18*, 1078–1082.
[28] Z. P. Liu, J. B. Liang, S. Li, S. Peng, Y. T. Qian, *Chem. Eur. J.* **2004**, *10*, 634–640.
[29] E. W. Radoslovich, M. Raupach, P. G. Slade, R. M. Taylor, *Aust. J. Chem.* **1970**, *23*, 1963–1971.
[30] N. Chakroune, G. Viau, S. Ammar, N. Jouini, P. Gredin, M. J. Vaulay, F. Fiévet, *New J. Chem.* **2005**, *29*, 355–361.
[31] Z. P. Liu, Y. Yang, J. B. Liang, Z. K. Hu, S. Li, S. Peng, Y. T. Qian, *J. Phys. Chem. B* **2003**, *107*, 12658–12661.
[32] L. Q. Zhang, A. K. Dutta, G. Jarero, P. Stroeve, *Langmuir* **2000**, *16*, 7095–7100.

Received: June 15, 2006
Published Online: October 10, 2006

